

# ABOUT GRADIENT OPERATORS ON HYPERSPECTRAL IMAGES

Ramón Moreno and Manuel Graña

*Computational Intelligence Group, University of the Basque Country, San Sebastián, Spain*

**Keywords:** Hyperspectral, Hyperspherical coordinates, Gradient, Chromatic Edge, Shadows.

**Abstract:** Gradient operators allow image segmentation based on edge information. Gradient operators based on chromatic information may avoid apparent edges detection due to illumination effects. This paper proposes the extension of chromatic gradients defined for RGB color images to images with n-dimensional pixels. A spherical coordinate representation of the pixel's content provides the required chromatic information. The paper provides results showing that gradient operators defined on the spherical coordinate representation effectively avoid illumination induced false edge detection.

## 1 INTRODUCTION

Edge detection is a key step in some image segmentation process. Edges are customarily computed by applying linear gradient operators (i.e. Sobel, Prewitt, Canny (Wang, 1997; Hildreth, 1987; Gonzalez & Woods, 1992)). In color images, gradients operators can be applied to each image dimension independently, combining the results afterwards. Alternatively, k-means clustering can be applied to obtain color regions, defining the edges as the boundaries of the found regions. The definition of gradient operators on multi-dimensional pixel images is an open research issue (Cheng, Jiang, Sun, & Wang, 2001). Some approaches try to exploit the properties of the color space (RGB, HSI, HSV, CIE  $L^*a^*b$ , CIE  $L^*u^*v$ ) to obtain sensible edge detections. Chromatic gradient operators have been proposed on the basis of the spherical representation of the color points (Moreno, Graña, & Zulueta, 2010). Higher dimension images, hyperspectral images, are becoming more common due to the lowering cost of hyperspectral cameras, and the growing number of airborne and satellite hyperspectral sensors deployed by a number of agencies. The issue of edge detection and the effect of shadows and highlights is also open in this kind of images. In many cases, shadows are hand annotated in the remote sensing images to prevent miss-segmentation. Chromaticity concepts have not been extended to the hyperspectral image domain so

far, though they can be useful to improve segmentation results. This paper proposes the hyperspherical coordinate representation of the n-dimensional Euclidean space (Moreno et al., 2010) in order to introduce images. Hyperspherical coordinate color representation allows to separate chromaticity and intensity, the main colorimetric separation, without changing the image space. It is therefore possible to extend Prewitt-like gradient operators defined on the image pixels' chromaticity (Moreno et al., 2010) to the hyperspectral case. Those operators are independent of the image luminosity, avoiding false edge detection on highlights and shadows in the hyperspectral case.

This paper is outlined as follows: in Sec. 2 we discuss about the Hyperspherical coordinates, giving in 2.1 the transformation from Euclidean coordinates to Hyperspherical coordinates. After that, in Sec. 3 we discuss about gradients, and in Sub-sec.3.1 we will present a chromatic gradient operator. In Sec. 4 we will show the experimental results, finishing this work in Sec. 5 with the conclusions.

## 2 HYPERSPHERICAL COORDINATES AND CHROMATICITY

An n-sphere is a generalization of the surface of an ordinary sphere to an n-dimensional space. n-Spheres are named Hyperspheres when

dimensionality is bigger than 3. We are interested in the hyperspherical representation of an hyperdimensional point and its implications for image segmentation under a chromatic point of view. In a three-dimensional color space, like RGB, figure 1 shows the spherical representation of a color point. A color  $c$  with (r,g,b) coordinate values in RGB color space can be represented by spherical coordinates  $(\theta, \phi, l)$ , where  $\theta$  and  $\phi$  are the angular parameters and  $l$  the vector magnitude.

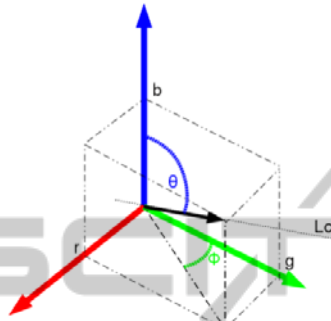


Figure 1: A vectorial representation of color  $c$  in the RGB space.

Spherical coordinates in the three-dimensional RGB color space can be used to estimate the illumination source chromaticity, and to detect chromatic edges (Moreno, Graña, & d'Anjou, 2011; Moreno et al., 2010). In the three-dimensional RGB color space, there is a direct correspondence between angular parameters  $(\theta, \phi)$  and chromaticity (Moreno et al., 2011). The angular parameters define a line which is the natural characterization of the pixel chromaticity. In other words, all points on this line have the same chromaticity with the pixel. The spherical expression of a point in Euclidean space allows to separate intensity and chromaticity, where  $l$  is the intensity, and the angular parameters provide a representation/codification of the pixel's chromaticity.

### 2.1 Hyperspherical Coordinates

Let us denote  $p$  hyperspectral pixel color in  $n$ -dimensional Euclidean space. In Cartesian coordinates it is represented by  $p = \{v_1, v_2, v_3, \dots, v_n\}$  where  $v_i$  is the coordinate value of the  $i$ -th dimension. This pixel can be represented in Hyperspherical coordinates  $p = \{l, \phi_1, \phi_2, \phi_3, \dots, \phi_n\}$ , where  $l$  is the vector magnitude that gives the radial distance, and  $\{\phi_1, \phi_2, \phi_3, \dots, \phi_n\}$  are the angular parameters. This coordinate transformation is performed uniquely by the following expression, for all cases except the ones described below:

$$\begin{aligned}
 l &= \sqrt{v_1^2 + v_2^2 + v_3^2 + \dots + v_n^2} \\
 \phi_1 &= \text{arccot} \frac{v_1^2}{\sqrt{v_2^2 + v_3^2 + \dots + v_n^2}} \\
 \phi_2 &= \text{arccot} \frac{v_1^2}{\sqrt{v_3^2 + v_4^2 + \dots + v_n^2}} \\
 &\vdots \\
 \phi_{n-2} &= \text{arccot} \frac{v_{n-2}^2}{\sqrt{v_{n-1}^2 + v_n^2}} \\
 \phi_{n-1} &= 2 \text{arccot} \frac{\sqrt{v_{n-1}^2 + v_n^2} + v_{n-1}}{v_n}
 \end{aligned}$$

Exceptions: if  $v_i \neq 0$  for some  $i$  but all of  $v_{i+1}, v_{i+2}, \dots, v_n$  are zero then  $\phi_i = 0$ . When all  $v_1, \dots, v_n$  are zero then  $\phi_i$  is undefined, usually a zero value is assigned.

A more compact notation for the hyperspherical coordinates is  $p = \{l, \bar{\phi}\}$  where  $\bar{\phi}$  is the vector of size  $n-1$  containing the angular parameters. Given a hyperspectral image  $I(x) = \{(v_{i+1}, v_{i+2}, \dots, v_n)_x ; x \in \mathbb{N}^2\}$ , where  $x$  refers to the pixel coordinates in the image domain, we denote the corresponding hyperspherical representation as;  $P(x) = \{(l, \bar{\phi})_x ; x \in \mathbb{N}^2\}$ , from which we use  $\bar{\phi}_x$  as the chromaticity representation of the pixel's and  $l_x$  as its (grayscale) intensity.

To clarify the meaning of the chromaticity in the hyperspectral image domain, we give an illustrative example. We have generated a synthetic hyperspectral image of  $5 \times 5$  pixels and 200 spectral bands. Each pixel spectral signature has the same Gaussian shaped profile but with different peak height, corresponding to different image intensity as can be appreciated in Fig. 2(a) showing the image intensity  $l_x$ . Fig. 2(b) shows the spectral signature of all pixels in the Cartesian coordinate representation, Fig.2(c) shows the chromatic spectral signature  $\{\bar{\phi}_x\}$  which is the same plot for all pixels. The chromaticity  $\bar{\phi}$  thus defines a line in the  $n$ -dimensional space of hyperspectral pixel colors of points that only vary their luminosity  $l$ .

According to the foregoing coordinate transformation, we can perform the following hyperspectral separation. Given a hyperspectral image  $I(x) = \{(v_{i+1}, v_{i+2}, \dots, v_n)_x ; x \in \mathbb{N}^2\}$  in the traditional Cartesian coordinate representation we can compute the equivalent hyperspherical representation  $(x) = \{(l, \bar{\phi})_x ; x \in \mathbb{N}^2\}$ . Then, we can

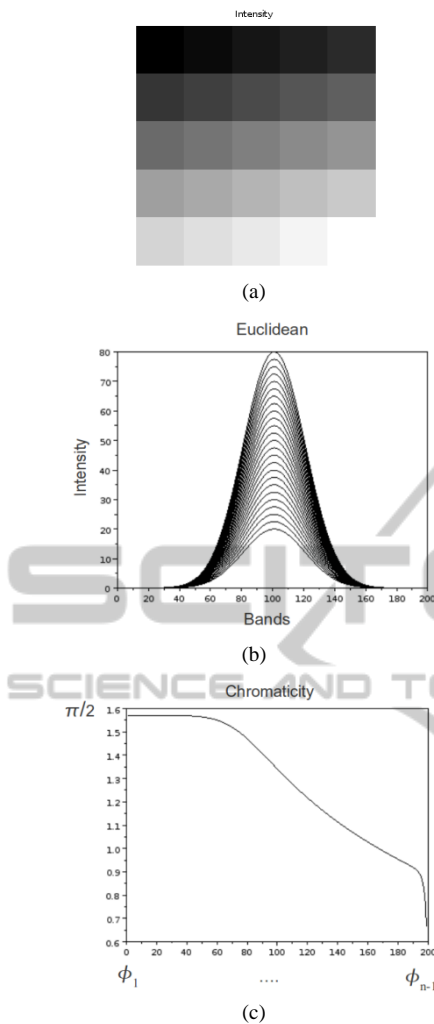


Figure 2: Synthetic image (a) the image intensity  $I_x$ , (b) shows the Gaussian shaped signature profile of all the pixels, and (c) shows the angle components of the Hyperspherical coordinates shared by the spectral signatures of all pixels in the image, corresponding to the common chromaticity of the pixels.

construct the separate intensity image  $L(x)$  in Fig (a). This separation allows us the independent processing of hyperspectral color and intensity information, so that segmentation algorithms showing color constancy can be defined in the hyperspectral domain. This decomposition can be also embedded in models of reflectance like the Dichromatic Reflection Model (Shafer, 1984) of the Bidirectional Reflection Distribution Function where they can be decomposed as diffuse and specular components.

### 3 GRADIENT OPERATORS

Mathematically, the gradient of elements of a bidimensional space domain function (like images) is given at each image domain point by the function derivative given by its horizontal and vertical Cartesian coordinates, which are the partial derivatives in these directions. Partial derivatives are often computed by linear convolution operators. The gradient function measures the rate of change of the function in a point. Gradients are easily computed on the intensity image, but their extension to high dimensional images is an open research issue.

Let us denote  $x = (i, j)$  the pixel coordinates in the image domain. We recall the definition of the image spatial gradient:

$$\nabla I(i, j) = \begin{bmatrix} G_i(i, j) \\ G_j(i, j) \end{bmatrix} = \begin{bmatrix} \frac{\partial}{\partial i} I(i, j) \\ \frac{\partial}{\partial j} I(i, j) \end{bmatrix}$$

where  $I(i, j)$  is the image intensity function at pixel  $(i, j)$ . For edge detection, the usual convention is to examine the gradient magnitude:

$$G(i, j) = |G_i(i, j)| + |G_j(i, j)|$$

For color images, a simplistic approach to perform edge detection is to drop all color information, and convolve the intensity image with a pair of high-pass convolution kernels to obtain the gradient components and gradient magnitude. The simplest edge detectors are the Prewitt detectors, is illustrated in Fig.3 because we will build our own spatial chromatic gradient operators following their pattern. To take into account spectral information, the straightforward approach is to apply the gradient operators to each spectral band as an independent intensity image and to combine the results afterwards  $\nabla I = \sum_1^n \nabla I_i / n$  where  $I_i$  denotes the  $i$ -th image spectral band.

$$\begin{bmatrix} -1 & 0 & 1 \\ -1 & 0 & 1 \\ -1 & 0 & 1 \end{bmatrix} \begin{bmatrix} -1 & -1 & -1 \\ 0 & 0 & 0 \\ 1 & 1 & 1 \end{bmatrix}$$

Figure 3: Prewitt mask.

Fig. 4 shows the results of this approach using Prewitt gradient operators on two hyperspectral images (The first one is a plastic blue ball in front of a green background, the second one is a plastic orange ball in front of the same green background. Both images captured under natural sun illumination). The first row shows one band of the images. Second row shows the gradient magnitude.

The third row shows some edges detected applying a threshold to the gradient magnitude image. The intensity image component has a strong influence on this gradient computation, therefore some highlights and shadows are identified as image regions and their boundaries detected as image edges.

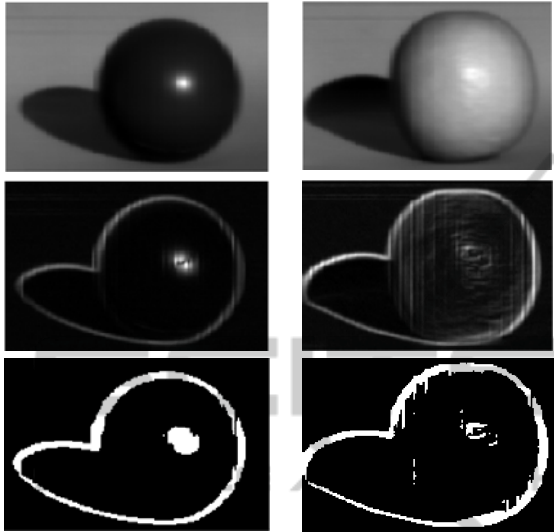


Figure 4: Results on two hyperspectral images of image gradient computed applying the Prewitt gradient operators to each band independently.

### 3.1 Chromatic Gradient Operator

Linear convolution gradient operators, such as the Prewitt operators shown in Fig. 4, the underlying topology is the one induced by the Euclidean distance defined on the Cartesian coordinate representation. In order to define a chromatic gradient operator, we may assume a kind of non-linear convolution where the convolution mask has the same structure as the Prewitt operators, but the underlying chromatic distance is based only on the chromaticity as follows: For two pixels  $p$  and  $q$  we compute the Manhattan or Taxicab distance on the chromatic representation of the pixels:

$$\angle(p, q) = \sum_{i=1}^{n-1} |\bar{\Phi}_{p,i} - \bar{\Phi}_{q,i}|$$

Note that the  $\angle(\mathbf{C}_p, \mathbf{C}_q)$  distance is always positive. Note also that the process is non linear, so we can not express it by linear convolution kernels. The row pseudo-convolution operator is defined as

$$CR_R(\mathbf{C}(i, j)) = \sum_{r=-1}^1 \angle(\mathbf{C}_{i-r, j+1}, \mathbf{C}_{i-r, j-1})$$

and the column pseudo-convolution is defined as

$$CR_C(\mathbf{C}(i, j)) = \sum_{c=-1}^1 \angle(\mathbf{C}_{i+1, j-c}, \mathbf{C}_{i-1, j-c})$$

so that the color distance between pixels substitutes the intensity subtraction of the Prewitt linear operator. The hyperspectral chromatic gradient magnitude image is computed as:

$$CG(x) = CR_R(x) + CR_C(x) \quad (1)$$

## 4 EXPERIMENTAL RESULTS

Experiments are performed on images taken by SOC 710 hyperspectral camera. Spectral resolution is 128 bands in the range 300nm to 1000nm. These images have been presented in the first row of Fig. 4. On these images we can analyze the illumination effects over the objects. On these images there are only two chromatically different surfaces, a uniform green background and a monochromatic object, in one case a dark blue ball with a sweet surface; in the other one is plastic model of an orange. In the second case, the object has a wrinkled surface.

We have applied the chromatic gradient of eq. 1 on the images. The results are shown in Fig. 5 First row shows the original intensity images. The second row shows the chromatic gradient magnitude image. As we can appreciate, true surface edges are better detected than in Fig.4 even on shadowy regions of the image. The highlights have lower response than in Fig.4, so that no spurious edges are detected around them. The chromatic gradient has a high response on the shadows, but this response is uniformly distributed on the whole shadow and it is not bigger than the true borders. This effect is consequence of the noise distribution on the image. The chromatic distance is more sensitive on region with poor illumination or on regions poor reflectance like the blue ball. Comparing these results with the traditional gradients like the shown on Fig.4, the chromatic gradient is focused on the chromaticity and has a bigger response on chromatic edges. Finally, last row shows the edge detection after applying a threshold on the gradient magnitude image. The threshold is computed by the Otsu minimal variance approach. In these results, we have found the correct object edges avoiding the false detection of borders of shines and shadows despite the high dimensional nature of these hyperspectral images.

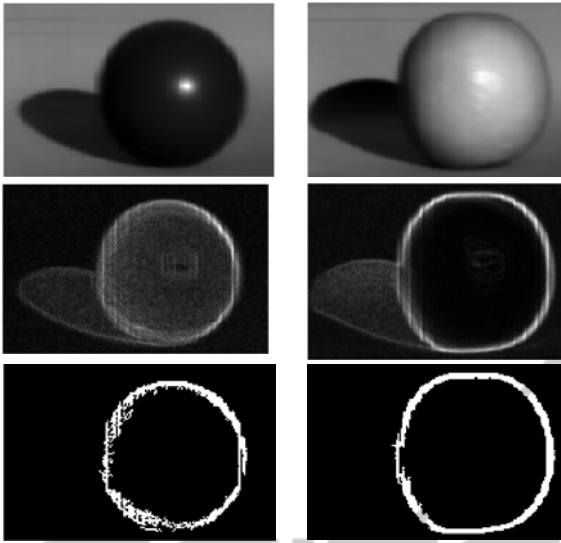


Figure 5: Pseudo Prewitt gradient on the chromatic image.

## 5 CONCLUSIONS

The computation of gradients on hyperspectral images implies the combination of high dimensional information and is prone to spurious detections due to noise and illumination effects, such as highlights and shadows. We have followed the approach proposed in (Moreno et al., 2010) for color images, proposing an extension to high-dimensional images, which allows the robust detection of object boundaries despite strong illumination effects. We have tested the approach on indoors captured hyperspectral images. Object boundaries are effectively found and spurious edges are avoided in these images. Further work on the extensive validation of the approach on hyperspectral images with known ground truth is on the way. Long term research goal is its application to remote sensing images.

## REFERENCES

- Cheng, H., Jiang, X., Sun, Y., & Wang, J. (2001, Dec). Color image segmentation: advances and prospects. *Pattern Recognition*, 34(12), 2259–2281.
- Gonzalez, R. C., & Woods, R. E. (1992). Digital image processing (3rd ed.). Addison-Wesley Pub (Sd).
- Hildreth, E. C. (1987). Computations underlying the measurement of visual motion. In (pp. 99–146). Norwood, NJ, USA: Ablex Publishing Corp.
- Moreno, R., Graña, M., & d'Anjou, A. (2011). Illumination source chromaticity estimation based on spherical coordinates in rgb. *Electronics Letters*, 47(1), 28-30.

Moreno, R., Graña, M., & Zulueta, E. (2010, Jun). RGB colour gradient following colour constancy preservation. *Electronics Letters*, 46(13), 908–910.

Shafer, S. A. (1984, april). Using color to separate reflection components. *Color Research and Applications*, 10, 43-51.

Wang, D. (1997, Dec). A multiscale gradient algorithm for image segmentation using watersheds. *Pattern Recognition*, 30(12), 2043–2052.